Type II detwinning in NiTi

Tawhid Ezaz and Huseyin Sehitoglu[a)]
Department of Mechanical Science and Engineering, University of Illinois, 1206 West Green Street, Urbana, Illinois 61801, USA

(Received 31 January 2011; accepted 14 March 2011; published online 5 April 2011)

Shape memory effect in nickel-titanium (NiTi) alloys depends on phase transformation between two phases and growth of twin variants in martensite called detwinning. An outstanding issue regarding detwinning in NiTi has been the lack of fundamental understanding of its mechanism at the atomistic level. The present article resolves this issue via first-principles energetics calculations of twin nucleation and growth. Our results based on ion relaxation and valence charge distribution point to a distinct energy barrier during detwinning process and the mechanism is mediated by a complex conjunction of shear and shuffle. © *2011 American Institute of Physics*.
[doi:10.1063/1.3574775]

The near equiatomic shape memory alloy nickel-titanium NiTi has attracted considerable attention.[1] The principle of shape memory effect relies on, (i) transformation between two phases of NiTi-high temperature austenite and low temperature martensite and (ii) the detwinning process observed in martensite during deformation. Austenite has a cubic lattice (B2) which transforms into multiple variants of monoclinic (B19′) martensite structure upon cooling. These particular variants are self-accommodating, and under deformation, reach a single variant state. This deformation process is different from dislocation mediated plastic deformation. In this work, we investigate the detwinning mechanism at the atomistic level by first-principles calculations and provide the energy barrier associated with the variant growth. Using density functional theory in NiTi martensite, we examine the bonding characteristics associated with detwinning and substantiate our findings with detailed energetics and valence charge redistribution.

Current understanding of the transformation twin systems is based on the phenomenological theory of martensite transformation proposed by Wechsler, Lieberman, and Read.[2] Detailed calculations indicate that nearly five types of transformation twin modes are possible. The experimental evidence shows that the most commonly observed transformation twins are Type II-1 type for solutionized NiTi.[3–7] Classical crystallographic theory suggests an irrational twin plane for Type II-1 twinning.[8] High resolution transmission electron microscopy investigations in NiTi confirmed that the irrational plane in type II-1 is comprised of rational ledges and step structures which reduce the total interfacial strain energy.[3,9,10] The interface of type II-1 twin between two variants A and B is shown in Fig. 1(a). During detwinning, type II-1 twin undergoes a collective movement of ledges and steps[3,10] and the variant A volume fraction increases [Fig. 1(b)].

The interplanar energy functional in a twinned system is termed the generalized planar fault energy (GPFE) curve.[11,12] A GPFE calculation requires shearing of consecutive elastic twin planes along the twinning shear direction relative to the pre-existing stacking fault or twin. However, a twinning shear alone may not be sufficient to generate a reflection twin and additional shuffles may be required[8] [Fig. 1(b)].

At the atomic level, the formation of a rational type II-1 twin in a martensite is accomplished by shear of Ni and Ti atoms in $(11\bar{1})$ planes in [011] direction.[3,7] In NiTi B19′, Ni, and Ti atoms cluster around a lattice point and create a motif unit. The twinning shear displaces the motif units to the twin position and an additional shuffle among the Ni atoms near the motif point completes the twin structure. Figure 1(b) illustrates the shear and shuffle mechanism during formation of a twin in martensite. To achieve a mirror reflection about [011] direction, additional shuffles are required for Ni atoms [shown with colored arrows in Fig. 1(b)]. The details of the simulation procedure are provided as a supplementary material.[13]

The predicted energy landscape for a five layer twin formation in NiTi martensite is plotted in Fig. 2(a). Unlike in

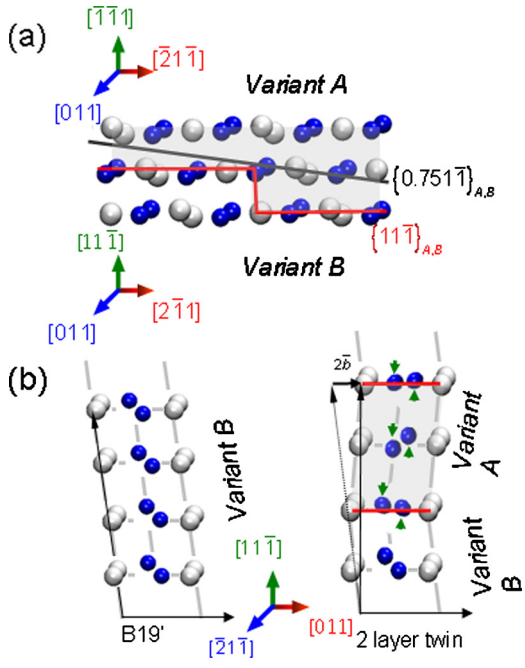

FIG. 1. (Color online) (a) Type II-1 twinning in NiTi corresponding to $(11\bar{1})[011]$ twin mode, the irrational twin plane and the step rational twin plane (b) Application of shear $(2\bar{b})$ and shuffle in ⟨205⟩ direction during twin growth in $(11\bar{1})[011]$ mode.

a)Author to whom correspondence should be addressed. Electronic mail: huseyin@illinois.edu.

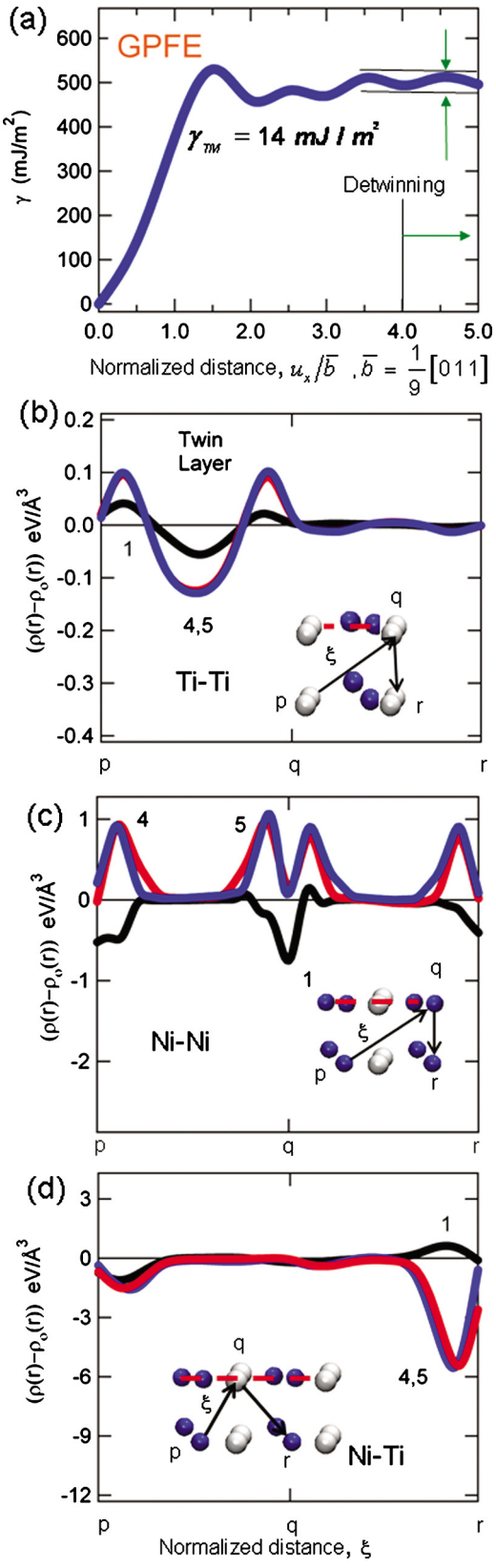

FIG. 2. (Color online) (a) GPFE for NiTi martensite in $(11\bar{1})[011]$ system versus normalized shear displacement on successive $(11\bar{1})$ plane; charge density difference between deformed and undeformed, (b) Ti–Ti atoms, (c) Ni–Ni, and (d) Ni–Ti under twinning shear 0.280 40 along path *p-q-r*.

fcc metals, the $u_x/\bar{b}=1$ is not a metastable position; hence, an intrinsic stacking fault is not possible in this system. Here, u_x and $\bar{b}$ correspond to the applied displacement and the total displacement respectively required for generating a one layer twin. However, we note that metastable positions are observed at $u_x/\bar{b}=2$ and at additional number of layers, $u_x/\bar{b}=3,4,5,\ldots$. Even though a two layer twin can be the smallest twin nucleus based upon the first metastable position, the GPFE illustrates that the twin stacking energy does not converge until the formation of a four layer twin. Consequently, the formation of type II-1 twin up to four layers can be best described as a twin nucleation process. The distinction between twin nucleation and twin growth is noteworthy since the stress required for twin growth is significantly lower.[14]

TABLE I. Deformation systems, fault energies and shear magnitudes.

Deformation mechanism	System	γ_{us} (mJ/m^2)	γ_{TM} (mJ/m^2)	Required shear strain (s)
Twin	$(11\bar{1})[011]$	530	14	0.2804
Slip	$(11\bar{1})[011]$	620[a]	⋯	1.21

[a]See Ref. 13.

During twin nucleation of a pristine variant, the barrier is 530 mJ/m^2 at $u_x/\bar{b}=1.5$. The barrier is exceptionally high, which explains the difficulty of deformation-induced twin nucleation. The GPFE curve in Fig. 2(a) shows fault energies remain unchanged with increase in twin thickness after the 4th layer twin. The steady oscillatory energy functional indicates the decoupling of the twin boundary effect. This energy barrier is termed the twin migration energy and is established as 14 mJ/m^2. This energy barrier is significantly lower than the twin nucleation barrier. Therefore, the energetics implies two separate mechanisms—(a) phase transformation induced twin nucleation and (b) deformation induced twin growth in martensite.

Twin growth in martensite in certain systems can be assisted by dislocation motion along the twin boundary.[15] Energy cost of dislocation motion is, thus, measured by shearing one elastic half space of $(11\bar{1})$ plane relative to the other in [011] shear direction (see Ref. 13, Fig. 1). However, no metastable energy well is observed up to a shear of magnitude 1.21; a possible intrinsic fault position. In addition to the high shear strain, the encountered unstable energy barrier is 620 mJ/m^2 (Table I). Because of this high barrier, dislocation glide is not favored in twinned martensite. Dislocations, however, can nucleate during austenite to martensite phase transformation[16] and play a role in compound {001}×⟨100⟩ twinning case.

Mechanical coupling in the GPFE curves originates from the bonding characteristics of Ni and Ti atoms. Electronic configuration of Ni and Ti is (Ar)$3d^8 4s^2$ and (Ar)$3d^2 4s^2$, respectively. Hence, partially occupied valence d bands lead to a weak directional bond in Ti. In the absence of hybridization, *s*-orbital leads to the formation of nondirectional bonds, which is manifested in Ni atoms.[17] The bonding characteristics under twinning shear can be investigated in terms of the valence charge density along a path *p-q-r* as shown in Figs. 2(b) and 2(c). The path is expressed in terms of ξ; where, ξ is the measured charge density position (x_i) along the path normalized by the bond distance pq or qr ($\xi_i = x_i/pq$ or $\xi_i = x_i/qr$). Here, atom q represents an atom in $(11\bar{1})$ plane at the growing twin boundary, whereas atom p and r lie one layer below in another $(11\bar{1})$ plane. Therefore,

the path *p-q* and *q-r* represents bonding characteristics of a boundary atom with its initial nearest neighbor and final nearest neighbor respectively after twinning shear. Charge density distributions of Ti–Ti, Ni–Ni, and Ni–Ti are plotted in terms of the difference between deformed and undeformed state, $[\rho(r)-\rho_o(r)]$, for *one*, *four*, and *five* layer thick twins. The plots exhibit a similar distribution for *four/five layer* twin and a distinct anomaly for *one layer* twin. Complete charge density isosurfaces of undeformed B19′ and *four layer* twin are given in supplementary Fig. 2.[13]

Under twinning shear, the maximum charge density distribution difference is observed at the halfway between two near neighboring Ti ions [Fig. 2(b)]. The distribution indicates that Ti–Ti bonds still maintain a weak directionality and breaking and reformation of directional bonds contribute to the overall deformation characteristics. In contrast, charge density distribution between Ni ions exhibits an accommodation process [Fig. 2(c)] which is observed in other metals with nondirectional metallic bonds.[18] Reverse charge density difference distribution in layer one and layers four/five plotted in Figs. 2(c) and 2(d) points to the shuffling of Ni atoms. Ni atoms, having nondirectional bonding between them, can squeeze like soft spheres and shuffle to a lower energy configuration state. Partial shuffling of Ni atoms is observed at the twin boundaries which has a significant contribution to the mechanical coupling between twin layers. Full shuffling of Ni atoms is observed in twinning after fourth layer growth of the twin. The direction and magnitude of full shuffle in Ni atoms are given in Supplementary Table II.[13] A significant nondirectional charge density difference is also prominent in Ni–Ti interactions [see, Fig. 2(d)], where a dissimilar pattern is also observed in one layer twin. The overall contribution of weak directional Ti–Ti, nondirectional Ni–Ni, and nondirectional Ni–Ti bonds results in bulk martensitic B19′ NiTi alloy exhibiting metallic bond attributes; this contrasts with austenitic B2 NiTi, which exhibit strong covalent bond characteristics.[17]

In this work, the detwinning mechanism of NiTi martensite has been addressed utilizing first principal calculations. The energetics reveal a clear distinction between nucleation and growth of type II-1 twinning. Shuffle, in addition to the lattice invariant shear, plays a vital role in the determination of twin migration energy.

The work is supported by the National Science Foundation under Grant Nos. DMR-0803270 and partially by CMMI-09-26813.

[1]K. Otsuka and X. Ren, Prog. Mater. Sci. **50**, 511 (2005).
[2]M. S. Wechsler, D. S. Lieberman, and T. A. Read, J. Met. **5**, 1503 (1953).
[3]K. M. Knowles, Philos. Mag. A **45**, 357 (1982).
[4]M. Nishida, K. Yamauchi, I. Itai, H. Ohgi, and A. Chiba, Acta Metall. Mater. **43**, 1229 (1995).
[5]T. Onda, Y. Bando, T. Ohba, and K. Otsuka, Mater. Trans., JIM **33**, 354 (1992).
[6]Y. Liu, Z. Xie, J. van Humbeeck, L. Delaey, and L. Yinong, Philos. Mag. A **80**, 1935 (2000).
[7]Z. L. Xie and Y. Liu, Philos. Mag. **84**, 3497 (2004).
[8]B. A. Bilby and A. G. Crocker, Proc. R. Soc. London, Ser. A **288**, 240 (1965).
[9]J. W. Christian, *The Theory of Transformations in Metals and Alloys* (Elsevier, Oxford, UK, 2002).
[10]Y. Liu and Z. L. Xie, Acta Mater. **51**, 5529 (2003).
[11]S. Hai and E. B. Tadmor, Acta Mater. **51**, 117 (2003).
[12]S. Kibey, J. B. Liu, D. D. Johnson, and H. Sehitoglu, Acta Mater. **55**, 6843 (2007).
[13]See supplementary material at http://dx.doi.org/10.1063/1.3574775 for materials and methods, lattice constants of B19′ NiTi, $(11\bar{1})[011]$ fault energy, and charge density plot.
[14]J. W. Christian and S. Mahajan, Prog. Mater. Sci. **39**, 1 (1995).
[15]Y. Kudoh, M. Tokonami, S. Miyazaki, and K. Otsuka, Acta Metall. **33**, 2049 (1985).
[16]T. Simon, A. Kröger, C. Somsen, A. Dlouhy, and G. Eggeler, Acta Mater. **58**, 1850 (2010).
[17]F. E. Wang, *Bonding Theory for Metals and Alloys* (Elsevier, Amsterdam, Netherlands, 2005).
[18]S. Ogata, J. Li, and S. Yip, Science **298**, 807 (2002).